(12) LEVEL II

(14) DNA 5159F-1

(6)

DELFIC: DEPARTMENT OF DEFENSE FALLOUT PREDICTION SYSTEM

Volume I - Fundamentals

Atmospheric Science Associates
P.O. Box 307
Bedford, Massachusetts 01730

(11) 31 Dec 1979

(12) 91

(1) Final Report for Period 16 Jan 1979—31 Dec 1979

CONTRACT No. DNA 001-76-C-0010

(15)

THIS WORK SPONSORED BY THE DEFENSE NUCLEAR AGENCY
UNDER RDT&E RMSS CODE B325076464 V99QAXNA01102 H2590D.

(16)

(17) H 211

Prepared for
Director
DEFENSE NUCLEAR AGENCY
Washington, D. C. 20305

temperature, or on default of input, the code will specify it. For this purpose we distinguish two types of soil: siliceous soil of continental (e.g., Nevada Test Site) origin (2200 ^{o}K), and calcarious soil of coral (e.g., Pacific Test Site) origin (2800 ^{o}K). On default of soil type specification, the code selects the continental type.

2.1.3 Mass and Geometry of the Cloud

On the basis of considerable experience with the cloud rise model we take the fraction of explosion energy used to heat air, soil and water to their initial temperatures to be 45% of the joule equivalent of the total yield, W. That is, the energy available to heat the cloud contents, H (joules), is

$$H = 0.45\ (4.18 \times 10^{12} W)$$

where W is in kilotons. To allow for situations where substantial amounts of water are taken into the fireball, the user may specify a number ϕ which is the fraction of H used to heat air and soil; the fraction $(1 - \phi)$ then is used to heat condensed water.

If the ambient temperature at the initial height of the cloud (eq. (2.1.13)) is $T_{e,i}$, then the masses of air and water in the cloud at t_i, $m_{a,i}$ and $m_{w,i}$(kg), are

$$m_{a,i} = \frac{\phi \left[H - m_s \int_{T_{e,i}}^{T_{s,i}} c_s(T)dT \right]}{\int_{T_{e,i}}^{T_i} c_{pa}(T)dT + x_e \int_{T_{e,i}}^{T_i} c_{pw}(T)dT} \qquad (2.1.7)$$

form of this equation results from a simple, approximate analysis of initial fireball rise, and the constant 1.2 is chosen to fit observed data. (Subroutine CRMINT)

2.1.5 Atmospheric Conditions

Height, radius and horizontal location relative to ground zero of the stabilized cloud* are sensitive to atmospheric stability and the ambient winds. The user provides single vertical profiles of atmospheric temperature, pressure, relative humidity and wind for use by the dynamic cloud rise. They also are used to compute particle settling and advection during the cloud rise such that by stabilization time, the particle cloud geometry is defined as functions of particle size and space above and downwind of ground zero. (Data input via subroutines ATMR and SHWIND)

Multiple wind profiles which may be used later for atmospheric transport (sec. 3.5) are not used here; a single wind profile is input especially for the cloud rise calculation.

In addition to pressure, temperature and humidity, the user also may input air density and viscosity, but in lieu of their input, the code computes them from the other quantities. Some flexibility of input is allowed: altitude, temperature and relative humidity must be specified, but either or both of pressure or density may be specified.

2.1.6 Particle Size Distribution

The user may specify one of three types of particle size distribution:

1. a lognormal distribution of number of particles with respect to diameter, specified in terms of median diameter and geometric standard deviation,

*Stabilization occurs when ambient transport and dispersion of the cloud becomes dominant over internally generated rise and expansion.

2. a power law distribution of particle mass fraction with respect to diameter, specified in terms of the power law exponent and a parameter k/m which is defined below, or

3. an arbitrary distribution of mass fraction with respect to particle diameter, specified by input of a table of values.

A lognormal distribution is selected by the code on default of user specification.

Lognormal Distribution[20]

The lognormal distribution is examined in some detail in Appendix A; here we present a brief summary. A particle distribution is said to be lognormal if the number of particles, $d\P(\delta)$, in the diameter range $d\delta$ centered on δ is given by

$$d\P(\delta) = \frac{1}{\sqrt{2\pi}\ \delta\ \ell n\ s}\ \exp\left[-\frac{1}{2}\left(\frac{\ell n\ \delta - \ell n\delta_{50}}{\ell n s}\right)^2\right] d\delta \qquad (2.1.15)$$

where δ_{50} and s are the median diameter and geometric standard deviation of the distribution.

For DELFIC calculations the user may specify δ_{50} and s*, or on default of specification, the code assigns the values

$$\delta_{50} = 0.407\ \mu m$$

$$s = 4.0\ ,$$

which are representative of Nevada Test Site fallout and are used for surface or near surface bursts ($\Lambda < 180$ ft $KT^{-1/3.4}$), while it assigns

*See Appendix A for a discussion of how to specify δ_{50} and s.

$$\delta_{50} = 0.15\ \mu m$$

$$s = 2.0$$

for pure air bursts ($\Lambda \geq 180$ ft $KT^{-1/3.4}$).[21]

A unique characteristic of the lognormal distribution is that the frequency functions for particle surface area and volume* are simply related to the frequency function for number. The surface area frequency with respect to diameter is obtained by replacing $\ell n\delta_{50}$ in eq. (2.1.15) with $\ell n\delta_{50} + 2(\ell ns)^2$, and the volume frequency by replacing $\ell n\delta_{50}$ in eq. (2.1.15) with $\ell n\delta_{50} + 3(\ell ns)^2$. Thus the median diameters for the surface and volume distributions corresponding to $\delta_{50} = 0.407\ \mu m$, $s = 4.0$ are 19 and 130 μm respectively, while those for $\delta_{50} = 0.15\ \mu m$, $s = 2.0$ are 0.39 and 0.63 μm. (Subroutines ICM and DSTBN)

Power Law Distribution

Power law distributions are mathematically meaningless since distribution functions cannot be defined for them. This is because the power law function is not properly bounded for zero argument. Freiling has shown that fallout particle distributions that have been represented by power law functions can equally well be fitted by lognormal distribution functions.[22] The implication of Freiling's work is that power law distributions would be more accurately described as truncated lognormal distributions. Nevertheless, power law distributions may be useful in fallout work.

Define the power law frequency as

$$d\pi(\delta|k,X) = k\delta^{-X}d\delta \quad , \tag{2.1.16}$$

where $d\pi(\delta|k,X)$ is the number of particles in the diameter range $d\delta$ centered on δ. If we assume spherical particles with constant density, ρ, we have

*Note that volume and mass distributions are equivalent for spherical particles whose densities are constant over the distribution.

$$dF\left(\delta \left| \frac{\pi\rho k}{6m_s}, X\right.\right) = \frac{\pi\rho k \delta^{3-X}}{6m_s}\, d\delta\,, \qquad (2.1.17)$$

where $dF\left(\delta \left| \frac{\pi\rho k}{6m_s}, X\right.\right)$ is the fraction of the total fallout mass, m_s, in the diameter range δ to $\delta + d\delta$.

The mass fraction of particles in the macro range from δ_i to δ_j is obtained by integration of eq. (2.1.17) between these limits to give

$$\Delta F = \frac{\pi\rho}{6(4-X)}\,(k/m_s)\left(\delta_j^{4-X} - \delta_i^{4-X}\right)\,, \quad 0 < X < 4. \qquad (2.1.18)$$

In DELFIC the power law distribution is specified by the exponential quantity X and the ratio k/m. Here we have dropped the subscript s from the mass since the ratio k/m would have been determined from one or more samples of fallout rather than from the entire mass of fallout. Details on data analysis and a description of the distribution in histogram form are given in Appendix B. (Subroutine DISTBN)

Tabular Distribution

Mass fraction and boundary particle diameters for each particle size class of a distribution histogram are specified by the user. The central particle diameter for the size class is taken to be the geometric mean of the boundary diameters. (Subroutine DSTBN)

Size-Activity Distribution

The user may specify any of the above to be a particle diameter-activity fraction distribution. For such a case the code selects an activity K factor (Roentgens m^2 hr^{-1} KT^{-1}) to match a user specified fission type, and a conventional, rather than rigorous, activity calculation ensues.

In effect this procedure also is used for pure air bursts, since DELFIC assumes that activity is uniformly distributed through the fallout particles, regardless of their size, for pure air bursts.

2.2 CLOUD RISE

2.2.1 Background

The DELFIC cloud rise model is based on the work of Huebsch[16,17] as modified by Norment.[8,13]. It provides a dynamic, one-dimensional, entraining bubble model of nuclear cloud rise, which is based on a set of coupled ordinary differential equations that represent conservation of momentum, mass, heat and turbulent kinetic energy. The nuclear cloud is defined in terms of: vertical coordinate of its center (the cloud is in some respects treated as a point),* cloud volume, average temperature, average turbulent energy density, and the masses of its constituents: air, soil and weapon debris, water vapor and condensed water. Cloud properties and contents are taken to be uniform throughout the cloud volume. The differential equations are solved by a fourth-order Runge-Kutta algorithm. (Subroutine RKGILL) Complete simulations use very little computer time.

Norment presents results of a validation study of the model.[13]

2.2.2 Differential Equations (Symbols are defined in the Glossary found in Appendix D.)

Momentum

$$\frac{du}{dt} = \overset{(a)}{\left(\frac{T^*}{T_e^*}\,\beta' - 1\right)}g - \overset{(b)}{\left(\frac{2k_2 v}{H_c}\,\frac{T^*}{T_e^*}\,\beta'\right)} + \overset{(c)}{\left(\frac{1}{m}\,\frac{dm}{dt}\right)}u \qquad (2.2.1)$$

*Effects of this model limitation on rise simulation of very large clouds are discussed in sec. 4 of ref. 13.

particle size distribution nor to distribute activity over this distribution. Complex calculations would be required to develop the information required and this work has not been done.

DELFIC uses a very rough procedure to correct for height of burst. This makes use of empirical data that relate fraction of total activity observed in local fallout to scaled height of burst.[35] In terms of the fraction of local surface burst activity observed, f_d, Showers[36] has expressed these data in the form

$$f_d = (0.45345)^{\lambda/65} \quad ; 0 < \lambda \tag{4.4.1}$$

where λ is scaled height of burst in terms of ft $KT^{-1/3}$. The fission yield is simply scaled down by this factor to correct for height of burst. Of course, if $\Lambda \geq 180$ (ft $KT^{-1/3.4}$), we assume that no local fallout occurs, and the pure air burst mode of calculation proceeds. (Subroutine OPM1)

6. VALIDATION

6.1 DISCUSSION

Predictions are compared with observed H + 1 hour normalized* exposure rate maps for the five test shots described in Table 2. The predictions were executed as discussed in reference 38, using the data listed there. Observed fallout patterns were taken from DASA 1251.

Three methods of comparison of fallout patterns are used here:

1. Visual comparison of contour maps.
2. Comparison of contour areas, and hotline lengths and azimuths.**
3. The Rowland-Thompson Figure-of-Merit (FM).[39] (Appendix C)

These are roughly in order of importance.

Statistical data are in Table 3 and the contour plots are on pp. 64 through 73. The contours were drawn by a 30-inch Calcomp plotter, and each observed-predicted pair are to the same scale.

TABLE 2

TEST SHOT DATA

Shot	Total Yield (KT)	Fission Yield (KT)	HOB (m)	Altitude of GZ (m)	Site
Johnie Boy	0.5	0.5	-0.584	1570.6	NTS+
Jangle-S	1.2	1.2	1.067	1284.7	NTS
Small Boy	low	-	3.048	938.2	NTS
Koon	150.	-	4.145	0.0	Bikini
Zuni	3380.	-	2.743	0.0	Bikini

+Nevada Test Site

*A "normalized" exposure rate map is constructed on the assumption that all local fallout is down at the specified time, regardless of its actual deposition time.

**Hotline length is defined as the furthest distance from ground zero on a contour, and hotline azimuth is the angle, measured clockwise from north, to the point of furthest distance from ground zero on a contour.

TABLE 3

COMPARISON OF OBSERVED AND PREDICTED FALLOUT PATTERN STATISTICS

Observed/Predicted

Test Shot	FM	Contour (Roentgen hr^{-1})	Area (km^2)	Hotline Length(km)	Azimuth (deg)
Johnie Boy	0.182	1000	0.278/0.029	1.38/0.32	359/0
		100	0.539/0.774	2.73/2.58	345/344
		50	1.271/1.787	4.10/4.13	343/343
			58(42)*	28(3)*	
Jangle-S	0.483	500	0.117/0.144	0.59/1.00	342/353
		300	0.386/0.316	1.50/1.23	346/354
		100	1.437/2.242	3.74/5.87	1/355
		35	3.114/5.077	5.06/7.68	6/355
			40(45)	43(42)	
Small Boy	0.308	1000	0.216/0.047	1.00/0.25	71/66
		500	0.528/0.135	1.62/0.56	73/80
		200	0.942/0.564	2.22/1.69	72/73
		100	3.75/1.10	5.66/3.72	72/74
		50	9.03/4.38	8.10/6.47	75/72
			63(59)	44(36)	
Koon	0.287	500	32.0/26.0	10.2 /12.5	18/0
		250	122/87.3	17.3 /24.2	15/4
		100	550/261	41.0 /39.5	17/3
			33(40)	22(22)	
Zuni	0.105	150	474/2239	98/78	12/337
		100	2761/3619	125/96	17/337
		50	6187/6660	138/121	27/338
		30	10950/9913	177/153	33/340
			105(16)	17(16)	

*Mean absolute percent errors. The value in parentheses is calculated without including the data for the highest activity level contour. See footnote next page.

Prediction accuracy is seen to be good, particularly for the low yield shots. Overall mean absolute percent errors* for contour area and hotline length are 61 and 32 percent respectively. If the data for the highest activity level contours are excluded, we have 42 and 26 percent for these errors. The highest level contours are particularly difficult to predict, usually being in the region affected by throwout and induced activity in and around the crater. DELFIC does not address this portion of the activity field since fallout is a negligible contributor to casualities there.

It is important to emphasize that this level of prediction competency is achieved without a posteriori adjustment or calibration of any aspect of the model such as to improve agreement with any observed fallout pattern.

The three low yield shots were executed at the Nevada Test Site, and their fallout patterns were measured over land. For this reason, observed patterns for these shots, though not highly accurate, may be considered to be superior to the patterns of the high yield shots which were executed on Bikini Atoll in the South Pacific. Not only are the fallout fields of the high yield shots very large, which adds to measurement problems, but most of the fallout from these shots fell into water. Even so, most of the Koon pattern area was covered by an array of fallout collection stations, so this pattern is probably reasonably accurate. Zuni, on the other hand, is a special case. The fallout pattern used here is exclusively downwind of the atoll and was determined by an oceanographic survey method that was known to be inaccurate. The close-in pattern in the region of the atoll is available, but contains no closed contours so could not be used here; thus the high-activity portion of the observed pattern for this shot is ignored, and this alone must account for a substantial portion of the disagreement

*For n observed-predicted data pairs, mean absolute percent error is

$$\frac{100}{n} \sum_{i=1}^{n} \left| x_{obs,i} - x_{pred,i} \right| / x_{obs,i} \quad .$$

between observation and prediction for this shot, particularly with regard to contour areas and overlap (Table 3). In addition, we have the following problem.

Predictions for these high yield shots are expected to be inferior to those for these low yield shots. This is because both of the high yield shots were detonated over coral soil, and in the case of Zuni, a large but uncertain amount of sea water was lifted by the cloud. The particle size distribution used for these predictions is typical of fallout produced from the siliceous soil found at the Nevada Test Site. We have not succeeded in developing a distribution appropriate for coral and coral-sea water mixtures.

More details concerning the prediction calculations and test shot characteristics are in reference 38.

6.2 OBSERVED AND PREDICTED FALLOUT PATTERNS

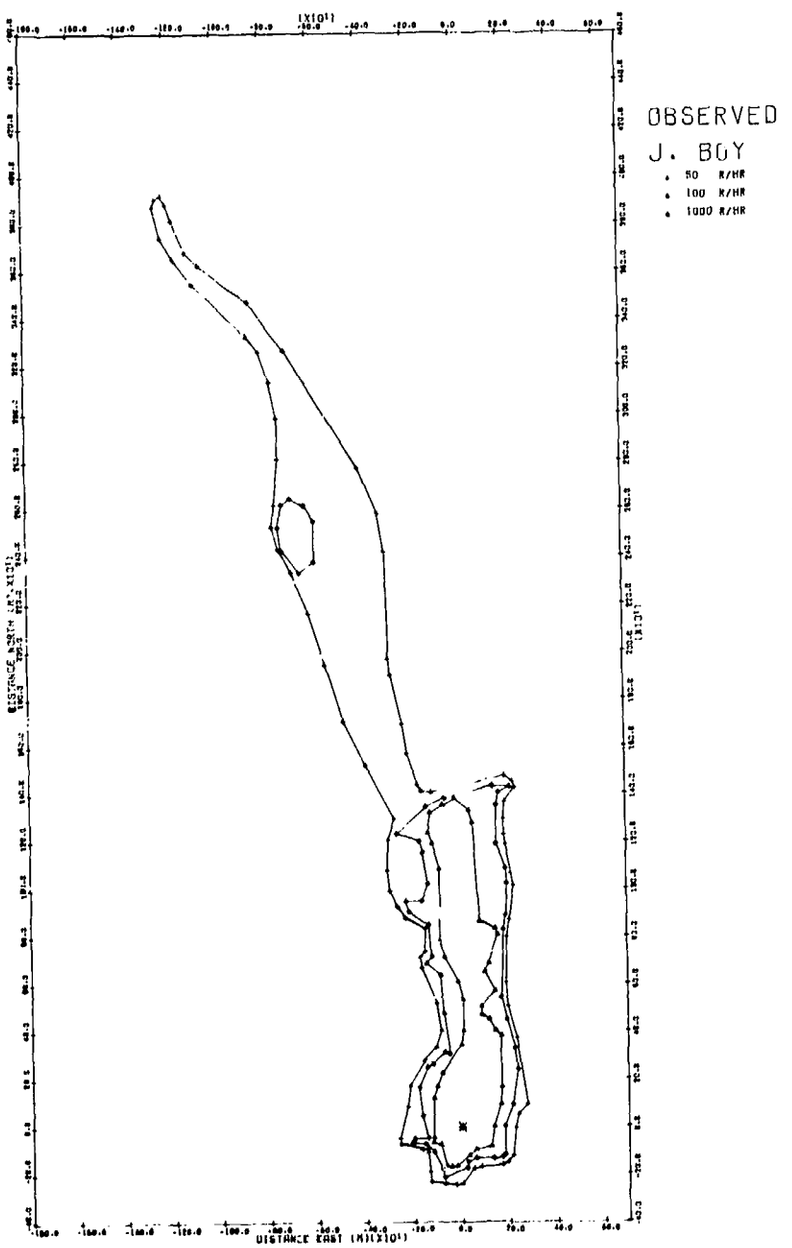

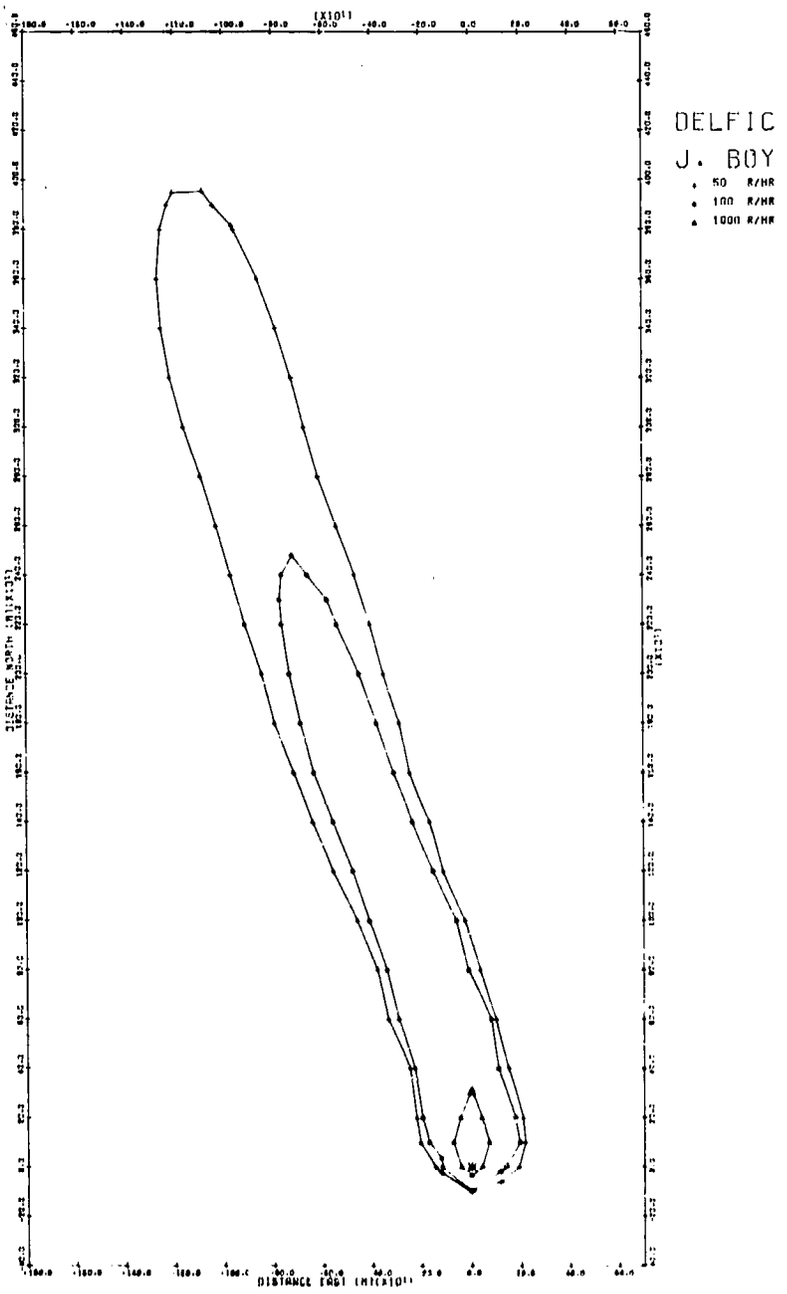
DELFIC
J. BOY
50 R/HR
100 R/HR
1000 R/HR

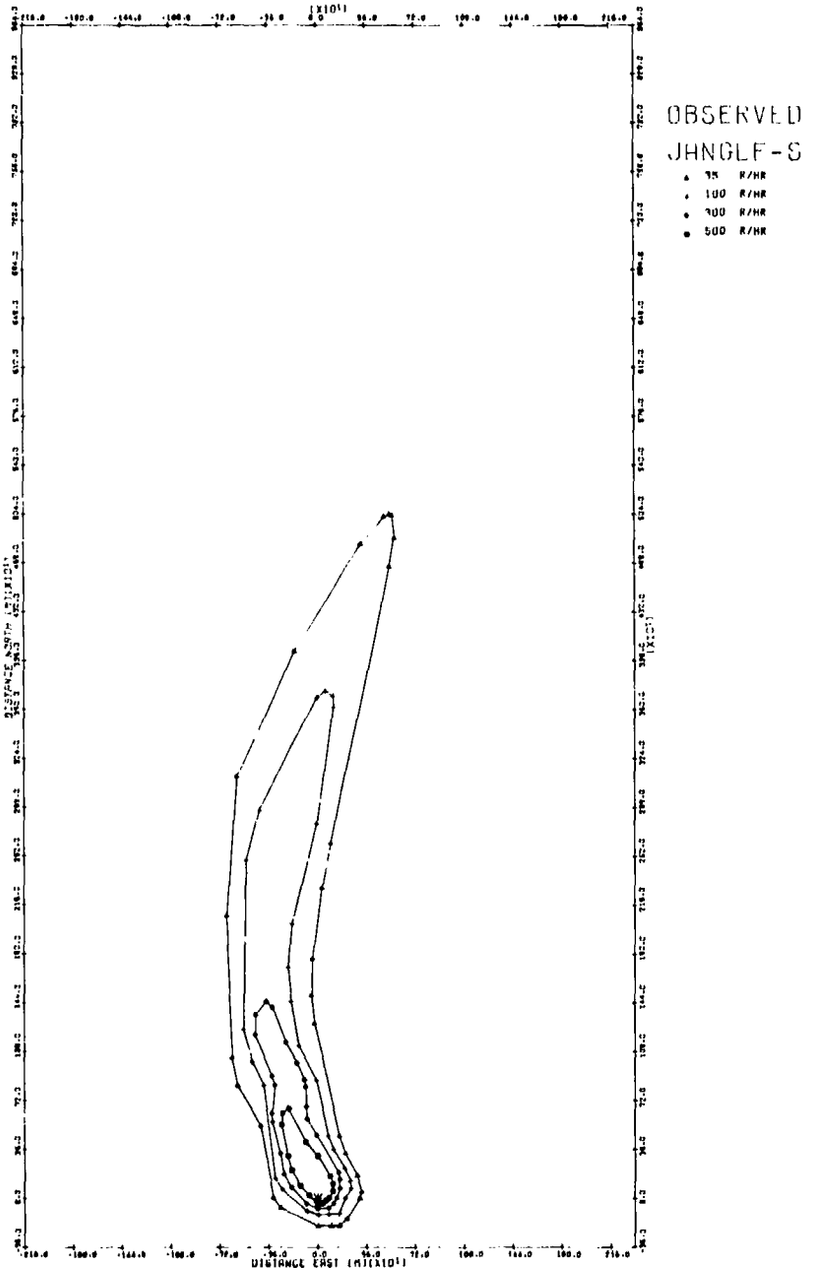
OBSERVED
JHNGLE-S
▲ 25 R/HR
• 100 R/HR
• 300 R/HR
● 500 R/HR
DISTANCE EAST (FT)(X10¹)

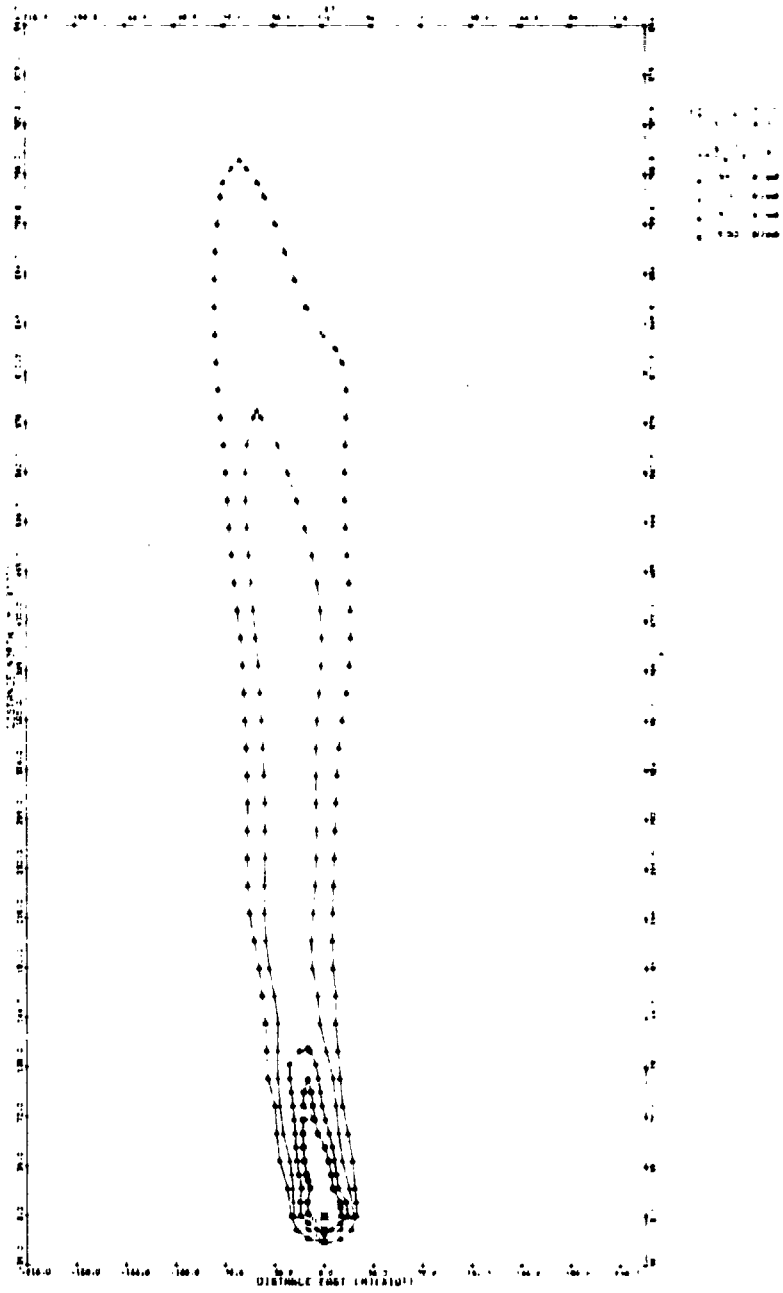

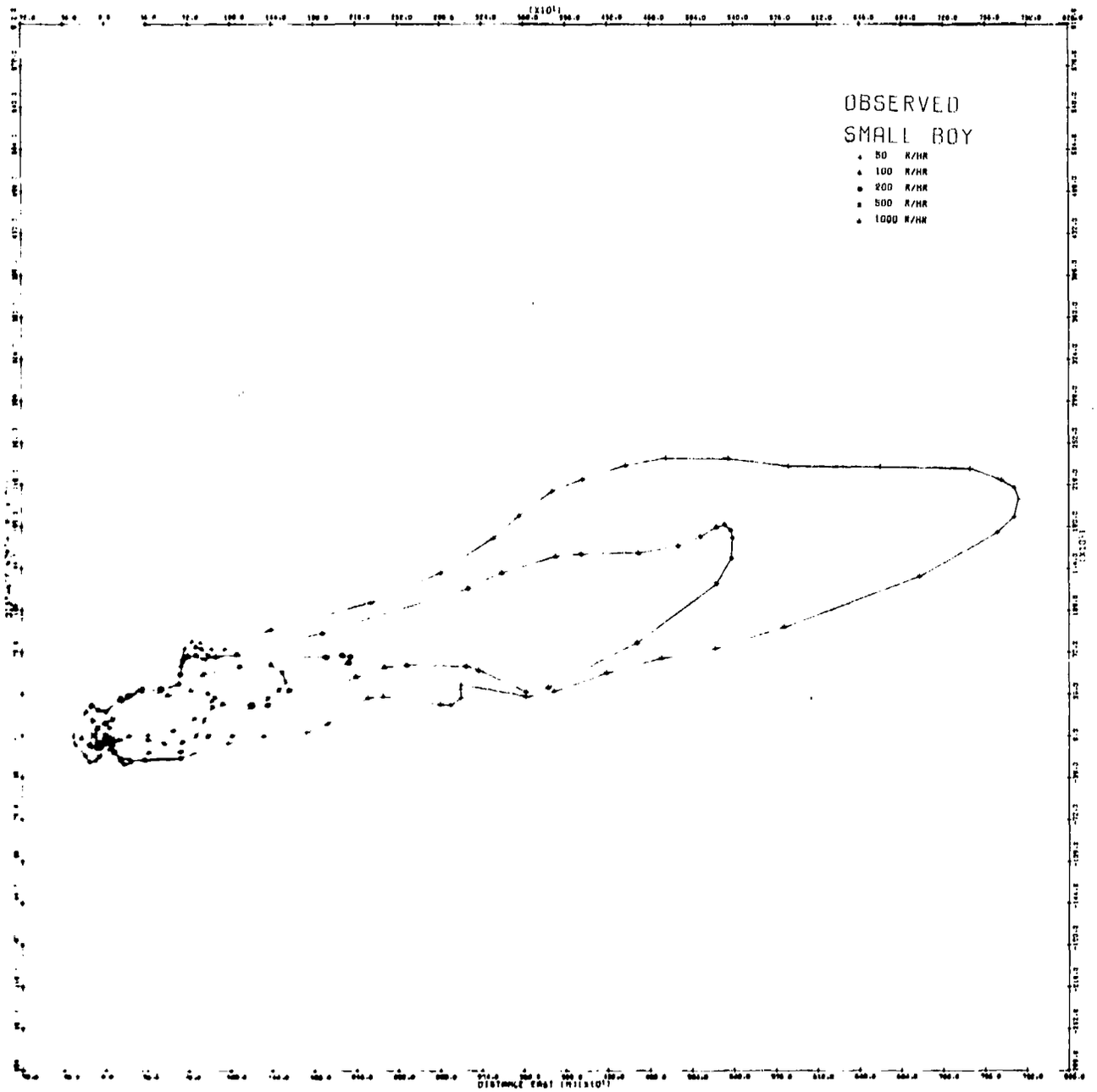
OBSERVED
SMALL BOY
50 R/HR
100 R/HR
200 R/HR
500 R/HR
1000 R/HR

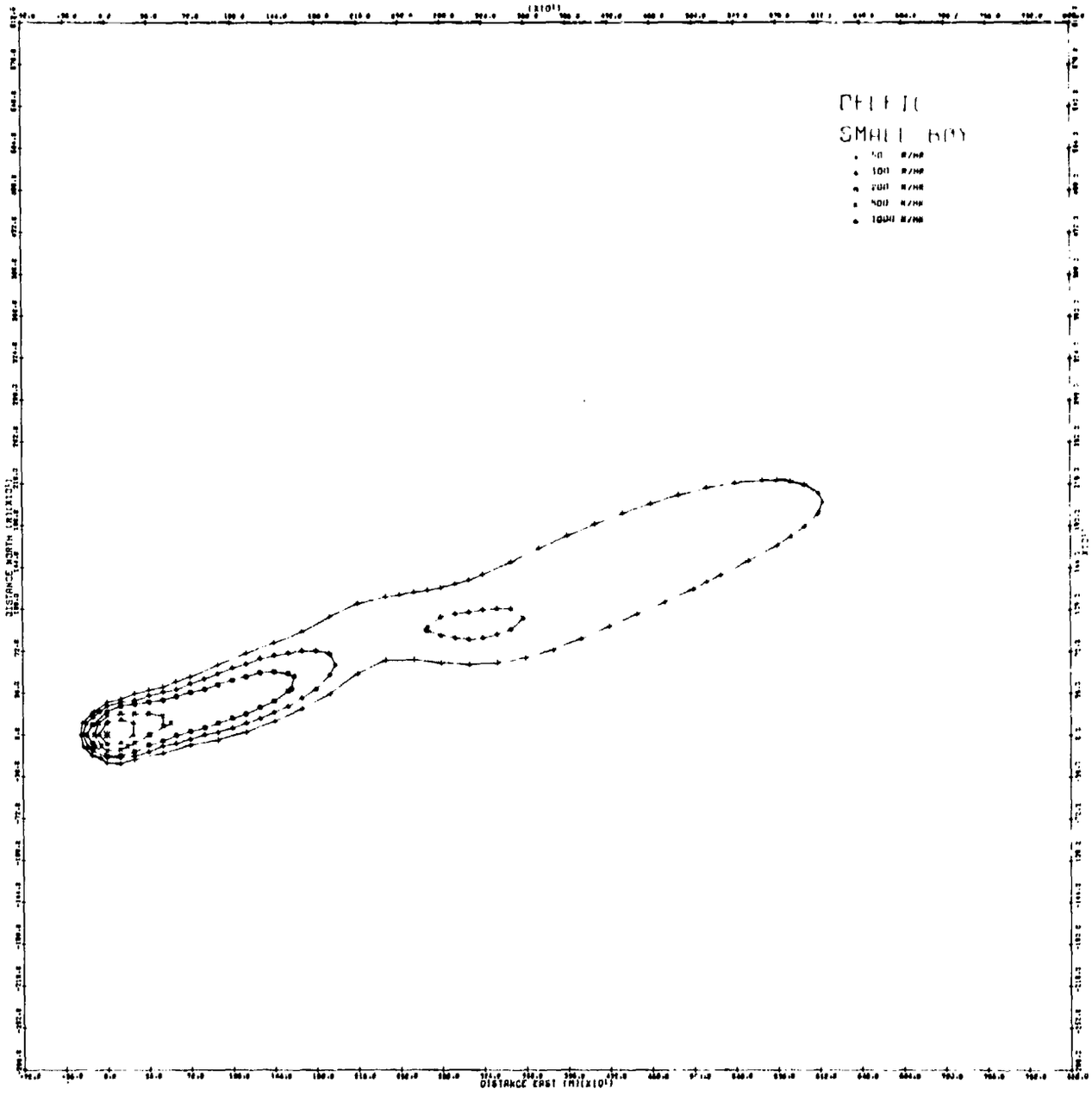
SMALL BOY
DISTANCE EAST (MI)(X10¹)

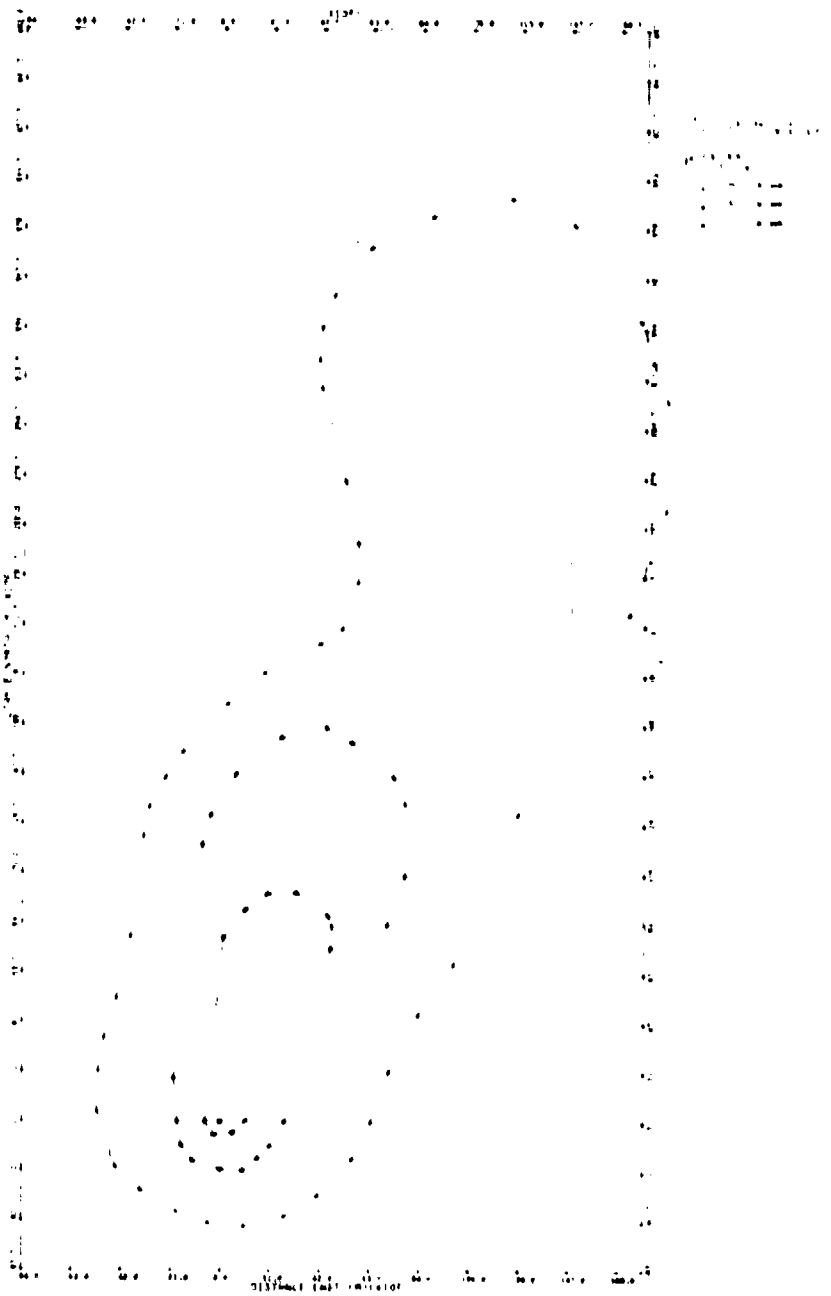

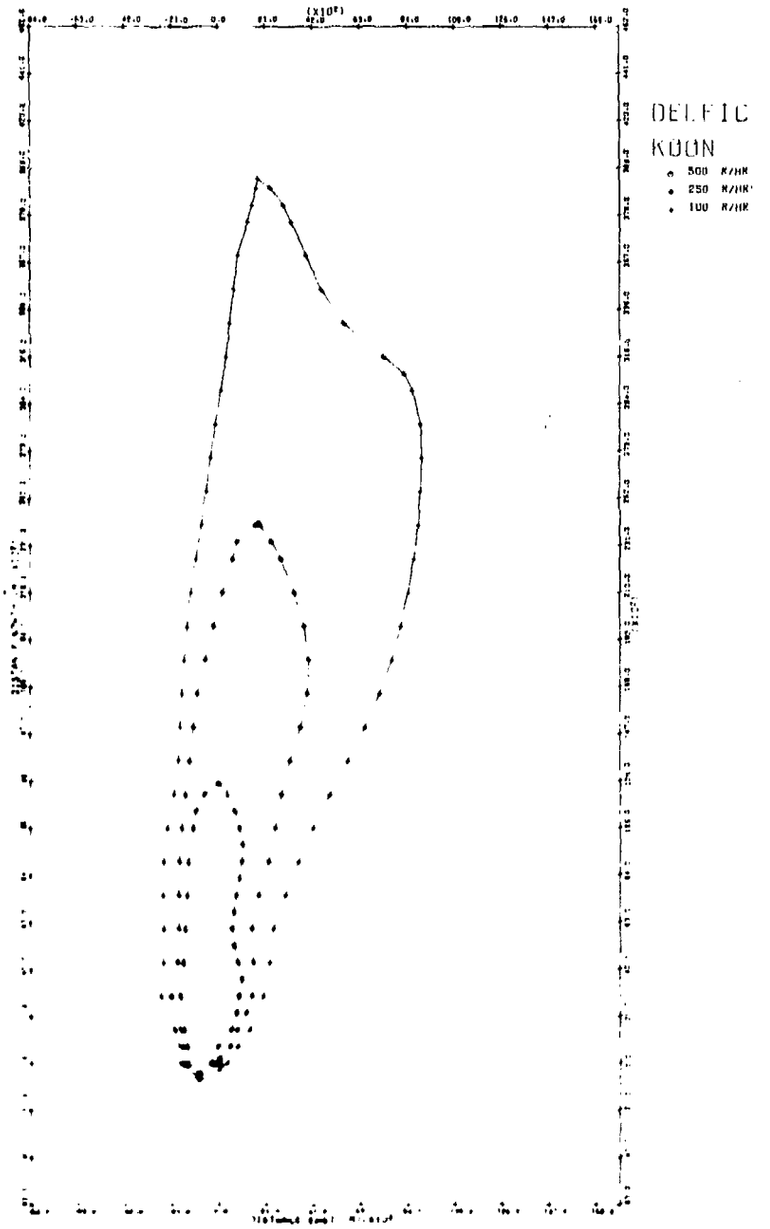
DELFIC
KOON
500 R/HR
250 R/HR
100 R/HR

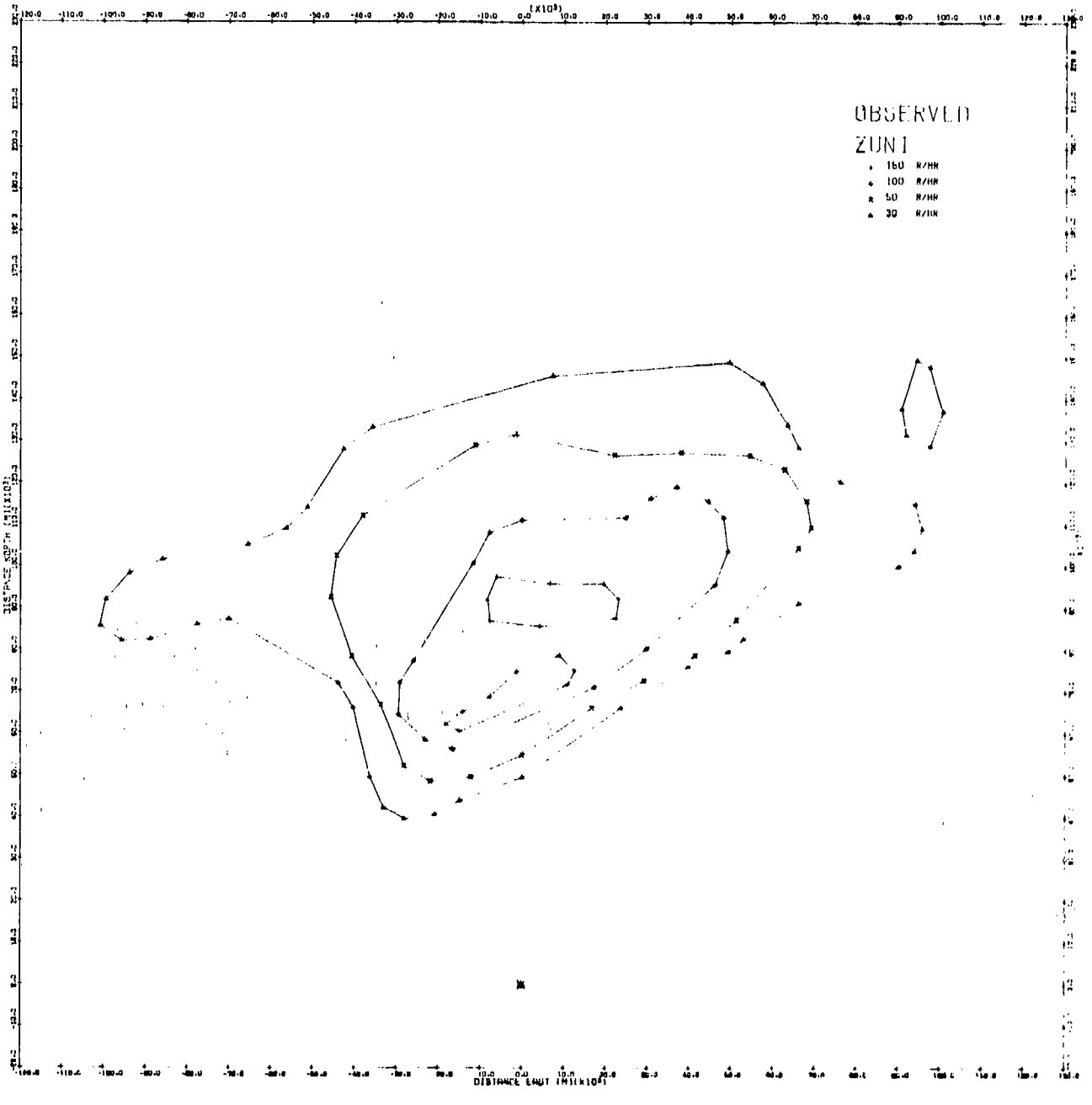
OBSERVED
ZUNI
150 R/HR
100 R/HR
50 R/HR
30 R/HR
DISTANCE EAST (MILES X10³)
DISTANCE SOUTH (MILES X10³)

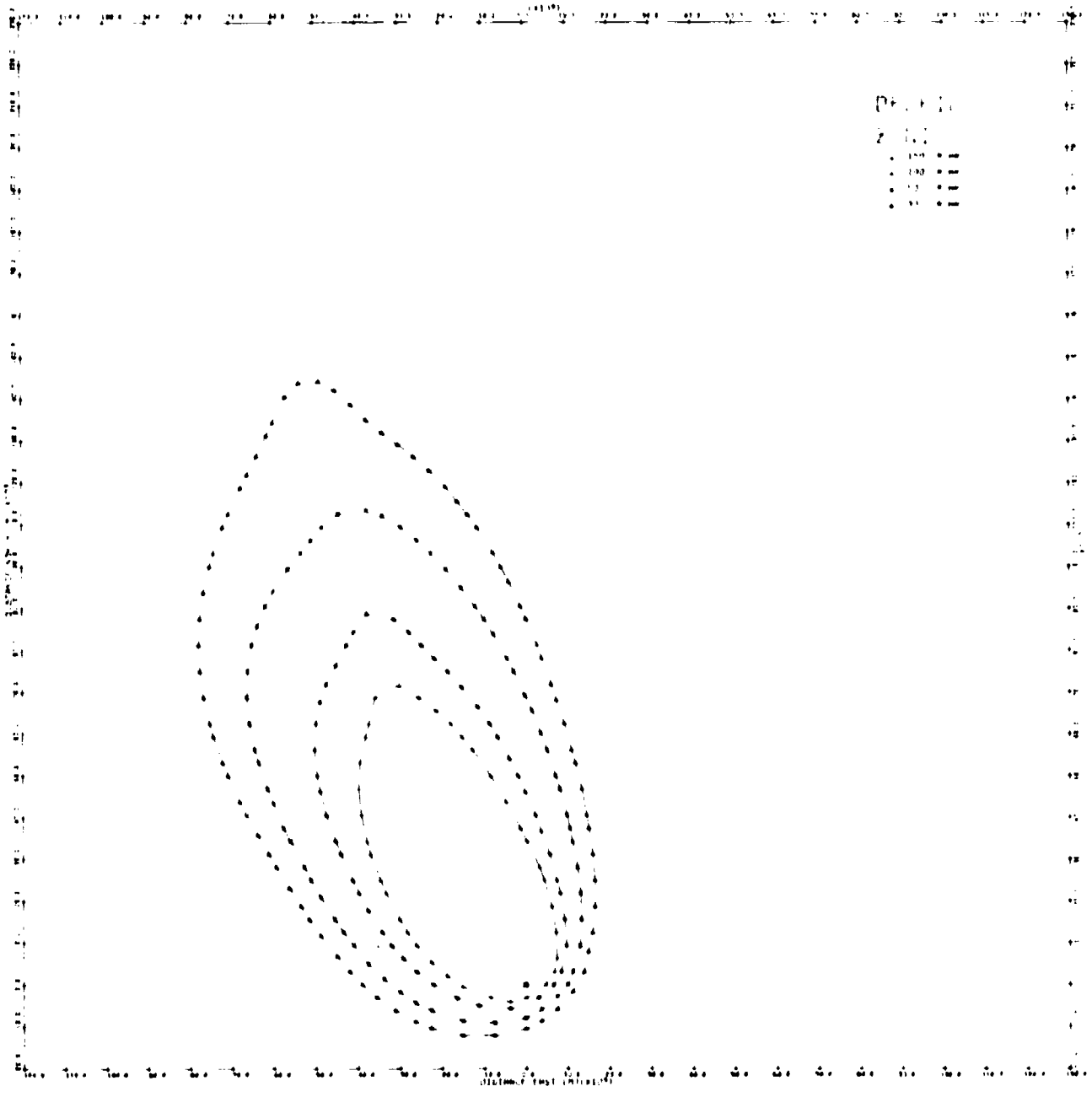

REFERENCES

1. H. G. Norment, "Department of Defense Land Fallout Prediction System, Volume I. System Description," Technical Operations Research, TO-B 66-40, DASA 1800-I (27 June 1966). AD- 483 897.

2. H. G. Norment, W.Y.G. Ing and J. Zuckerman, "Department of Defense Land Fallout Prediction System. Volume II. Initial Conditions," Technical Operations Research, TO-B 66-44, DASA 1800-II (30 September 1966). AD-803 144.

3. I. O. Huebsch, S. H. Cassidy, H. G. Norment, J. Zuckerman, and T. W. Schwenke, "Department of Defense Land Fallout Prediction System. Volume III, Cloud Rise," TO-B 66-45, DASA-1800-III (19 May 1967). AD-819 770.

4. H. G. Norment, T. W. Schwenke, I. Kohlberg and W.Y.G. Ing, "Department of Defense Land Fallout Prediction System. Volume IV. Atmospheric Transport," Technical Operations Research, TO-B 66-46, DASA-1800-IV, (2 February 1967). AD-815 263

5. R. C. Tompkins, "Department of Defense Land Fallout Prediction System, Volume V. Particle Activity," NDL-TR-102, DASA-1800-V (February 1968). AD-832 239.

6. T. W. Schwenke and P. Flusser, "Department of Defense Land Fallout Prediction System. Volume VI. Output Processor," TO-B 66-48, DASA-1800-VI (20 February 1967). AD-814 055.

7. D. K. Winegardner, "Department of Defense Land Fallout Prediction System, Volume VII. Operators' Manual," NDL-TR-104, DASA-1800-VII (April 1968). AD-836 871.

8. H. G. Norment and S. Woolf, "Department of Defense Land Fallout Prediction System, Volume III (Revised)," R70-1W. DASA-1800-III (Revised) (1 September 1970). AD-879 890.

9. H. G. Norment, "Department of Defense Land Fallout Prediction System, Volume II, Initial Conditions," DNA 1800-II (Supplement), (October 1972). AD-753 842.

10. H. G. Norment and E. J. Tichovolsky, "A New Fallout Transport Code for the DELFIC System: The Diffusive Transport Module." Arcon Corporation, R71-W, DASA-2669 (1 March 1971). AD-727 613. H. G. Norment, Mt. Auburn Research Associates, DNA-2669 - Supplement (October 1972). AD-751 542.

11. H. G. Norment, "A Revised Output Processor Module for the DELFIC Fallout Prediction System," DNA 2962F (October 1972). AD-751 543.

12. H. G. Norment, "A Precipitation Scavenging Model for Studies of Tactical Nuclear Operations. Vol. I: Theory and Preliminary Results. Vol. II: The DELFIC-PSM Code," DNA-3661F-1 and DNA-3661F-2 (May 1975) AD-014 960/9GI and AD-014 961/7GI.

13. H. G. Norment, "Validation and Refinement of the DELFIC Cloud Rise Module," Atmospheric Science Associates, DNA-4320F (15 January 1977) AD-A047 372.

14. M. D. Nordyke, "On Cratering: A Brief History, Analysis, and Theory of Cratering," Lawrence Radiation Laboratory, UCRL-6578 (22 August 1961).

15. H. G. Norment and W. Woolf, "Studies of Nuclear Cloud Rise and Growth," Technical Operations, Inc., unpublished.

16. I. O. Huebsch, "The Development of a Water-Surface-Burst Fallout Model: The Rise and Expansion of the Atomic Cloud," USNRDL-TR-741 (23 April 1964). AD-441 983.

17. I. O. Huebsch, "Turbulence, Toroidal Circulation and Dispersion of Fallout Particles from the Rising Nuclear Cloud," USNRDL-TR-1054 (5 August 1966).

18. K. V. Beard, "Terminal Velocity and Shape of Cloud and Precipitation Drops Aloft," J. Atm. Sci. 33, 851 (1976).

19. C. N. Davies, "Definitive Equations for the Fluid Resistance of Spheres," Proc. Phys. Soc. (London) 57, 259 (1945).

20. J. Aitchison and J.A.C. Brown, The Lognormal Distribution (Cambridge University Press, 1966).

21. M. W. Nathans, R. Thews, W. D. Holland and P. A. Benson, "Particle Size Distribution in Clouds from Nuclear Airbursts," J. Geophys. Res. 75, 7559 (1970).

22. E. C. Freiling, "A Comparison of the Fallout Mass-Size Distributions Calculated by Lognormal and Power-Law Models," USNRDL-TR-1105, U. S. Naval Radiological Defense Laboratory (14 November 1966). AD-646 019.

23. J. J. Walton, "Scale Dependent Diffusion," J. Appl. Meteor. 12, 547 (1973).

24. G. T. Csanady, "Turbulent Diffusion of Heavy Particles in the Atmosphere," J. Atm. Sci. 20, 201 (1963).

25. W. Y. Chen, "Energy Dissipation Rates in Free Atmospheric Turbulence," J. Atm. Sci. 31, 2222 (1974).

26. E. M. Wilkins, "Decay Rates for Turbulent Energy Throughout the Atmosphere," J. Atm. Sci. 20, 473 (1963).

27. E. H. Barker and T. L. Baxter, "A Note on the Computation of Atmospheric Surface Layer Fluxes for Use in Numerical Modeling," J. Appl. Meteor. 14, 620 (1975).

28. F. Pasquill, Atmospheric Diffusion, 2nd edition (Halsted Press, 1974).

29. D. Golder, "Relations Among Stability Parameters in the Surface Layer," Boundary-Layer Meteor. 3, 47 (1972).

30. G. P. Cressman, "An Operational Objective Analysis System," Monthly Weather Review 87, 367 (1959).

31. H. Bateman, "The Solution of a System of Differential Equations Occuring in the Theory of Radioactive Transformations," Proc. Cam. Phil. Soc. 15, 423 (1910).

32. T. H. Jones, "A Prediction System for the Neutron-Induced Activity Contribution to Fallout Exposure Rates," USNRDL-TR-1056, U.S. Naval Radiological Defense Laboratory (1966).

33. E. C. Freiling, "Fractionation I. High-Yield Surface Burst Correlation," USNRDL-TR-385, U.S. Naval Radiological Defense Laboratory (29 October 1959). AD-232 085.

34. E. C. Freiling, "Fractionation III. Estimation of Degree of Fractionation and Radionuclide Partition for Nuclear Debris," USNRDL-TR-680, U.S. Naval Radiological Defense Laboratory (September 1963). AD-423 725.

35. P. D. LaRiviere, et al., "Local Fallout From Nuclear Test Detonations. Vol. V. Transport and Distribution of Local (Early) Fallout From Nuclear Weapons Tests," unpublished.

36. R. L. Showers, "Improvements to the PROFET Fallout Prediction Program," Ballistics Research Laboratories, BRL-MR-2095 (February 1971). AD-883 280.

37. M. Abramowitz and I. A. Stegun, Handbook of Mathematical Functions, NBS-AMS 55 (June 1964).

38. H. G. Norment, "Evaluation of Three Fallout Prediction Models: DELFIC, SEER and WSEG-10," Atmospheric Science Associates, DNA 5285F (16 June 1978).

39. R. H. Rowland and J. H. Thompson, "A Method for Comparing Fallout Patterns," DASIAC, G. E. - Tempo. DNA 2919F (April 1972).